

GASTROINTESTINAL ABNORMALITIES IDENTIFIED BY FLUORESCENCE ENDOMICROSCOPY

HONGCHUN BAO*, ALEX BOUSSIOUTAS^{†,‡},
MCGEAREY ALEIXANDRIA[†], RITA BUSUTTIL[†] and MIN GU^{*,§}

**Center for Micro-Photonics
Faculty of Engineering and Industrial Sciences
Swinburne University of Technology
Hawthorn, Victoria 3122, Australia*

*†Research-Peter MacCallum Cancer Center
1 St Andrews Place
East Melbourne, Victoria 3002, Australia*

*‡Department of Medicine (RMH)
University of Melbourne, Royal Melbourne
Hospital, Parkville, Victoria 3050, Australia*

§mgu@swin.edu.au

Accepted 4 August 2012
Published 9 November 2012

Real-time *in vivo* microscopic imaging has become a reality with the advent of confocal and nonlinear endomicroscopy. These devices are best utilized in conjunction with standard white light endoscopy. We evaluated the use of fluorescence endomicroscopy in detecting microscopic abnormalities in colonic tissues. Mice of C57bl/6 strain had intraperitoneal injection with azoxymethane once every week for five weeks and littermates, not exposed to azoxymethane served as controls. After 14 weeks, intestines were imaged by fluorescence endomicroscopy. The images show obvious cellular structural differences between those two groups of mice. The difference in endomicroscopy imaging can be used for identifying tissues suspicious for neoplasia or other changes, leading to early diagnosis of gastrointestinal track of cancer.

Keywords: Endomicroscopy; fluorescence imaging; one-photon fluorescence imaging; gastrointestinal cancers; goblet cells; neoplasia.

1. Introduction

Cancer is one of the main causes of death in the world. But if they are detected early, most common cancers are easier to treat and cure.¹ By using a variety of screening tests, it is possible to prevent

and treat the disease long before symptoms appear. Gastrointestinal (GI) tract cancers, including oesophageal cancer, stomach cancer, gall bladder cancer, GI stromal tumors, liver cancer, pancreatic cancer, colon cancer, rectal cancer and anal cancer,

are the most common group of cancers. Detection of GI cancers at early stage is essential for the outcome of survival rate, which could increase by a factor of 5.¹

GI endoscopy, where a doctor is able to see the inside lining of the digestive tract, is the most effective method for GI disease detection.^{2,3} However, traditional endoscopy only measures organ surface morphology with image resolution on the order of 10 μm . Three-dimensional (3D) imaging of cellular layers and intracellular organs, which could be a very useful clue for early diagnosis of diseases, is missed by traditional endoscopy. Alternatively, biopsy has been used for GI cancer diagnosis.⁴ But the overall diagnostic accuracy by biopsy is limited by the fact that it cannot test all the samples needed to be surveyed and only a small portion of samples are tested.

Advances in this field have resulted in the development of new one-photon-excited fluorescence (OPF) or two-photon-excited fluorescence (TPF) endoscopy which could achieve 3D anatomical and functional fluorescence imaging of organs with high

resolution and visualize cellular-level details of tissue in real time without having to remove tissue.⁵⁻⁸ GI cancers begin when abnormal cells grow out of control and have a defined series of pre-malignant conditions which evolves with the accumulation of aberrant genetic events.⁹ These pre-malignant lesions have presented the change of the cell structure in tissue, which can be used for early diagnosis.¹⁰⁻¹² In this work, we use fluorescence endomicroscopy to detect those cell structure changes. Mice were induced with GI lesions by injecting a colon carcinogen. The cell architecture variation of the mice compared with the control mice is spotted by fluorescence endoscopy imaging of intestine of the mice. The cellular structure difference could be used for establishing a procedure of diagnosing GI cancers and determining the stage of their development.

2. Endomicroscopy

A laser source fluorescence endoscopy system (Fig. 1) was used for identifying the cell architecture

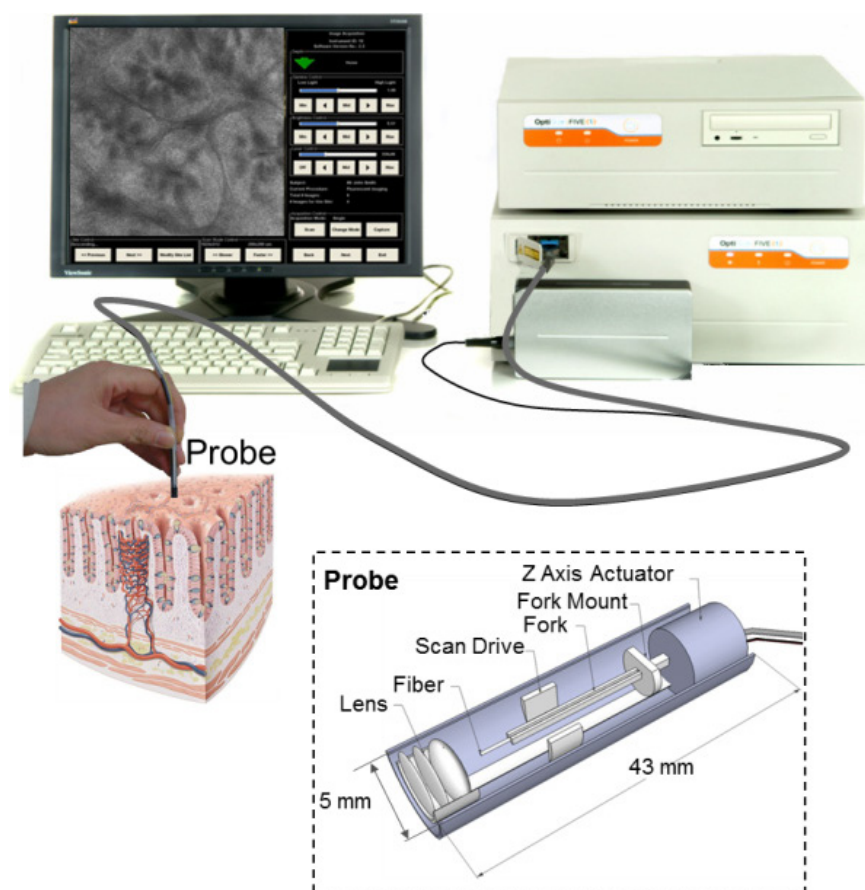


Fig. 1. OPF or TPF imaging endomicroscopy.

change at early stage of cancer. Figure 1 shows the schematic diagram of the fluorescence endomicroscope and the endoscopy probe. 3D OPF imaging and TPF imaging can be obtained through the same endomicroscopy system by using different lasers and optical fibers. A passive mode-locked Ti:Sapphire laser with a pre-chirp unit and a double clad fiber are employed for TPF imaging⁶⁻⁸ while a CW laser with a wavelength of 488 nm and a single mode fiber are used for OPF imaging.^{3,13} The laser beam is delivered from the laser source to the tested tissue by the optical fiber. A small endoscopy probe is attached to the end of the optical fiber. Inside the probe, a multiple element micro-lens focuses the laser beam delivered from the fiber to the samples. The end of the optical fiber is mounted on an electromagnetically driven resonant tuning fork which scans the optical fiber in the horizontal axis (Fig. 1, inset). The fork is also part of a cantilever, which provides vertical axis movement of the fiber tip. Raster scanning of fiber tip in horizontal (x) and vertical (y) axis is realized by the tuning fork. The image depth axis is controlled by a compact actuator based on shape memory alloy technology. 3D imaging with imaging volume $\geq 475 \times 475 \times 250 \mu\text{m}^3$ is achieved by the miniaturized probe. The fluorescence signal excited by the laser from the specimen is collected by the optical fiber and sent to a photomultiplier tube (PMT) for detection and displaying images. The micro-scanner and imaging display are

synchronized and controlled by electronic system in the control box.

3. Mouse Preparation

C57bl/6 strain black mice are used for the detection. Figure 2 shows the time line and how the mice were treated before imaging. The mice were divided into a test group and a control group. The test group of mice were injected with a colon carcinogen, azoxymethane (AOM), once every week for five weeks. At week five, both groups of mice were treated with dextran sulfate sodium salt (DSS) for 24 h. The mice were imaged by the endomicroscope on 2, July which is 14 weeks since initial AOM injection.

4. Imaging Results

The mouse was anesthetized and injected 0.3–0.4 ml of the fluorescein by tail vein injection (1% solution diluted in saline). After 5 min, when the fluorescein has been circulated around the whole body of the mouse, tissue was freshly harvested from the mouse body for endoscopic imaging. Figure 3 displays hematoxylin and eosin (H&E) image, OPF endoscopy image and TPF nonlinear image of large intestine of a mouse in the control group. The fluorescence endomicroscopy images show the luminal openings of the crypts and regular epithelial cells, where epithelial



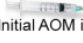



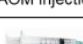
Time Line	Test mouse	Control mouse
		
26/03	 Initial AOM injection	No injection
01/04	 AOM injection 100 μl	No injection
08/04	 AOM injection 100 μl	No injection
15/04	 AOM injection 100 μl	No injection
22/04	 AOM injection 100 μl DSS treatment	No injection DSS treatment
02/07	Endoscopy imaging	Endoscopy imaging

Fig. 2. Time line for preparing the test mouse and the control mouse.

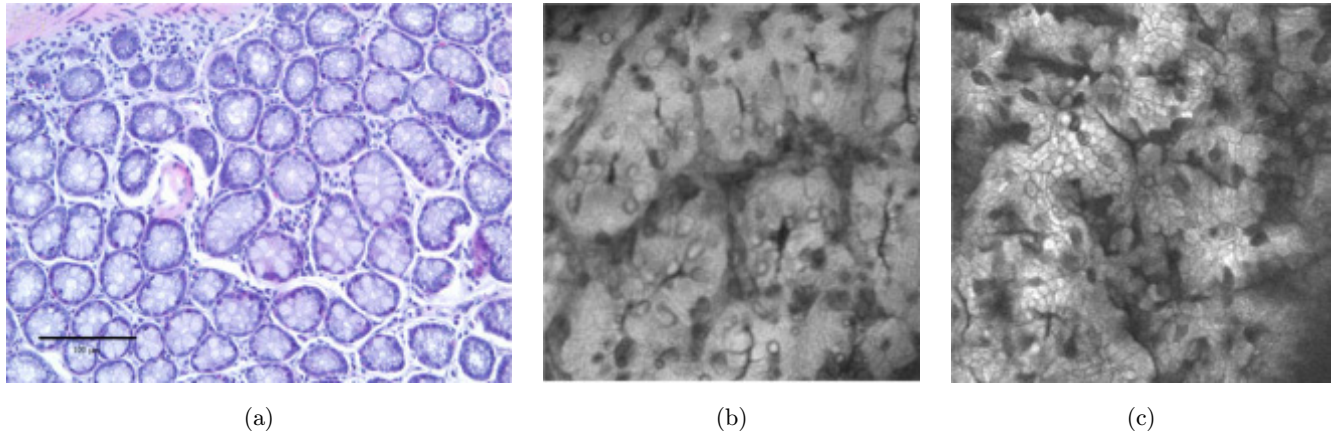


Fig. 3. Images of large intestine of a control mouse. (a) H&E image. (b) OPF image. (c) TPF image. Size of images (b) and (c): $200 \times 200 \mu\text{m}$.

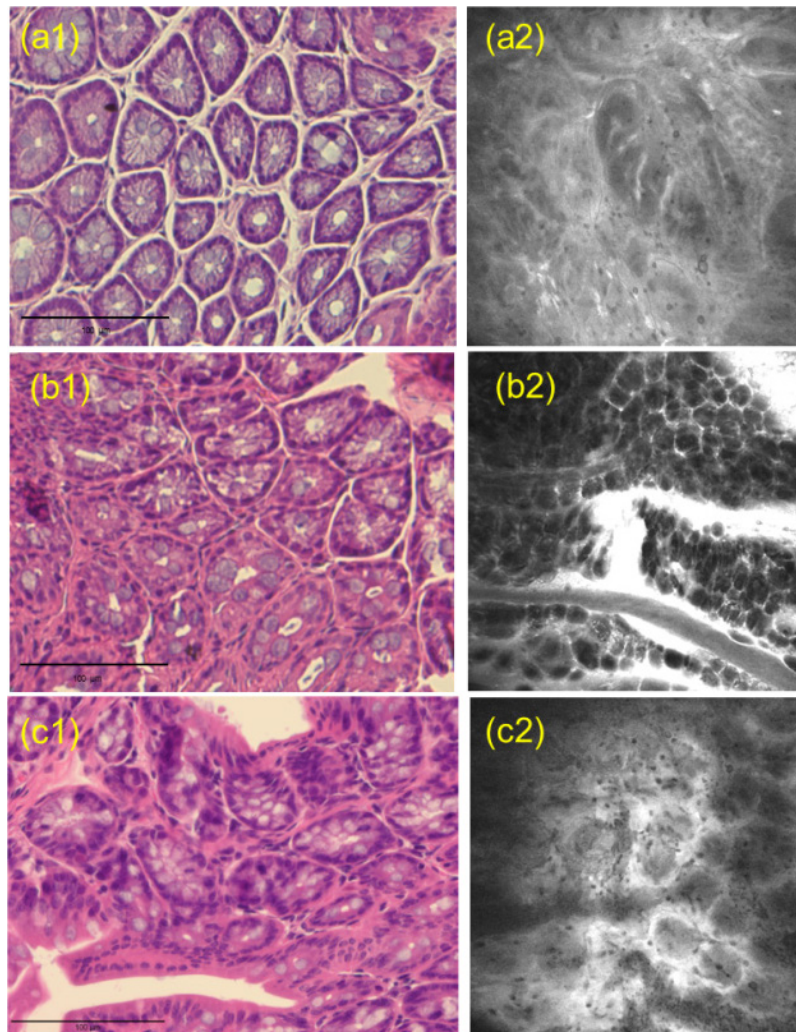


Fig. 4. H&E and OPF endomicroscopy images of large intestine of test mouse. (a2) Highly irregular glands and nuclei. (b2) Strong leakage with pooling of fluorescein within the lamina propria. (c2) Dysplasia of cell structure and leakage of fluorescein. Size of images (a2), (b2) and (c2): $475 \times 475 \mu\text{m}$.

columnar cells present as bright white cells. Goblet cells present as dark ovoids in the fluorescence images [Figs. 3(b) and 3(c)], and white ovoids at the H&E image [Fig. 3(a)]. Compared with Fig. 3(b), the TPF image [Fig. 3(c)] shows sharper subcellular structure and higher contrast. The image resolution of Fig. 3(c) was gained through nonlinear dependence of the fluorescence signal on excitation laser power in the two-photon excitation, while the fluorescence signal has linear relation with the excitation laser power in the one-photon excitation case. The high contrast [Fig. 3(c)] was due to the localization of the two photon excitation where the fluorescence signal only generated at focal spot of excitation laser beam and background noise from out of the focal area excitation was dramatically diminished.

Figure 4 displays H&E images and OPF images of large intestine of a mouse from the test group. Compared with Fig. 3(a), the H&E images do not show difference between a control mouse and a test mouse. However OPF images reveal obvious polyps and odd vascular on the surface of the tissue in Figs. 4(a2)–4(c2). Compared with Fig. 3(b), the border of the cells in Figs. 4(a2)–4(c2) becomes obviously blurred and cellular details in the images start to disappear. Figure 4(b2) displays crowds of dark cells of irregular size and leakage of fluorescein. Compared with Fig. 3(b), irregular crypt openings and disorganized cell architecture of the epithelial layer are obviously shown in Fig. 4(c2). Suspicious mucosal abnormalities are presented in the fluorescence endomicroscopy images.

5. Conclusion

Obvious cellular change of large intestine areas between the mouse in the test group with polyps induced by AOM injection and the mouse in the control group can be identified by fluorescence endomicroscopy. The images show that small and subtle dysplastic lesions can be detected by fluorescence endomicroscopy. Therefore, in conjunction with broad field techniques such as chromoendoscopy to identify regions of interest, it may provide a useful tool for early detection of cancers by identifying dysplasia. Identification of dysplasia using real-time techniques will enable targeted biopsies rather than more costly random biopsies used in screening for dysplasia of the colon in conditions such as inflammatory bowel disease.

Acknowledgments

The authors thank the Australian Research Council for its support and Optiscan Pty. Ltd. for providing FIVE1[®] OPF endomicroscopy and supporting the setup of TPF endomicroscopy.

References

1. K. Kinkel, Y. Lu, M. Both, R. S. Warren, R. F. Thoeni, "Detection of hepatic metastases from cancers of the gastrointestinal tract by using non-invasive imaging methods (US, CT, MR Imaging, PET): A meta-analysis," *Radiology* **224**, 748 (2002).
2. R. Soetikno, T. Kaltenbach, R. Yeh, T. Gotoda, "Endoscopic mucosal resection for early cancers of the upper gastrointestinal tract," *J. Clin. Oncol.* **23**, 4490 (2005).
3. R. Kiesslich, P. R. Galle, M. F. Neurath, *Atlas of Endomicroscopy*, Springer Medizin Verlag Heidelberg (2008).
4. T. Itoi, Y. Shinohara, K. Takeda, K. Takei, H. Ohno, K. Ohyashiki, N. Yahata, Y. Ebihara, T. Saito, "Detection of telomerase activity in biopsy specimens for diagnosis of biliary tract cancers," *Gastrointest. Endosc.* **52**, 380 (2000).
5. B. A. Flusberg, E. D. Cocker, W. Piyawattana-metha, J. C. Jung, E. L. M. Cheung, M. J. Schnitzer, "Fiber-optic fluorescence imaging," *Nat. Methods* **12**, 941 (2005).
6. H. Bao, J. Allen, R. Pattie, R. Vance, M. Gu, "A fast handheld two-photon fluorescence micro-endoscope with a $475\ \mu\text{m} \times 475\ \mu\text{m}$ field of view for *in vivo* imaging," *Opt. Lett.* **33**, 1333 (2008).
7. H. Bao, A. Boussioutas, R. Jeremy, S. Russell, M. Gu, "Imaging of goblet cells as a marker for intestinal metaplasia of the stomach by one-photon and two-photon fluorescence endomicroscopy," *J. Biomed. Opt.* **14**(6), 064031 (2009).
8. M. Gu, H. Bao, J. L. Li, "Cancer-cell microsurgery using nonlinear optical endomicroscopy," *J. Biomed. Opt.* **15**, 050502 (2010).
9. Y. Otani, I. Okazaki, M. Arai, K. Kameyama, N. Wada, K. Maruyama, K. Yoshino, M. Kitajima, Y. Hosoda, M. Tsuchiya, "Gene expression of interstitial collagenase (matrix metalloproteinase 1) in gastrointestinal tract cancers," *J. Gastroenterol.* **29**, 391 (1994).
10. H. Zeng, A. Weiss, R. Cline, C. E. MacAulay, "Real-time endoscopic fluorescence imaging for early cancer detection in the gastrointestinal tract," *Bioimaging* **6**, 151 (1998).
11. L. Mao, M. P. Schoenberg, M. Scicchitano, Y. S. Erozan, A. Merlo, D. Schwab, D. Sidransky,

- “Molecular detection of primary bladder cancer by microsatellite analysis,” *Science* **271**, 659 (1996).
12. R. Jain, L. Munn, D. Fukumura, “Dissecting tumour pathophysiology using intravital microscopy,” *Nat. Rev. Cancer* **2**, 266 (2002).
 13. M. Goetz, C. Fottner, E. Schirmacher, P. Delaney, S. Gregor, C. Schneider, D. Strand, S. Kanzler, B. Memadathil, E. Weyand, M. Holtmann, R. Schirmacher, M. M. Weber, M. Anlauf, G. Klöppel, M. Vieth, P. R. Galle, P. Bartenstein, M. F. Neurath, R. Kiesslich, “*In-vivo* confocal real-time mini-microscopy in animal models of human inflammatory and neoplastic diseases,” *Endoscopy* **39**, 350 (2007).